DOI 10.5162/EUROSENSORS2025/TP51

Integrating Carbon Nanotube Strain Gauges onto Stretchable PDMS Patches for Respiration Activity Sensing

Stefanie Jucker[1], Morten Vollmann[1], Cosmin Roman[1], Signe Lin Vehusheia[1], Mainak Basu[1], Christofer Hierold[1]
[1] ETH Zurich, Tannenstrasse 3, 8092 Zürich, Switzerland
croman@ethz.ch

Summary:
In this work we demonstrate the integration of a solid-state carbon nanotube strain gauge onto a soft, stretchable PDMS patch. We have designed, simulated and characterized the mechanical response of these devices. White-light interferometry is utilized to characterize the mechanical deformation suffered upon assembling the strain gauges onto the patches, and to determine key parameters such as the leverage factor η (1.25 nm/µm) which captures the strain transfer from the patch to the individual carbon nanotube strain gauge. Simulations show that η can be tuned by design for customizable sensitivity.

Keywords: Carbon nanotubes, PDMS, Stretchable patches, Strain sensing, Wearable sensors

Background and Motivation

Piezoresistive sensors based on individual carbon nanotubes (CNTs) have demonstrated excellent gauge-factors, ultra-low power consumption and very small footprints [1]. These features are promising for wearable biomedical devices. Also, the tiny mass of CNTs makes them insensitive to body motion artifacts. Several groups have developed stretchable strain sensors based on CNT-containing films. For instance, layers containing CNTs have been printed onto PDMS substrates, achieving up to 45% stretchability with gauge factors (GF) ~36 for wearable strain sensors [2]. Such devices are low-cost and achieve excellent stretchability. Their GFs are typically <100, but only at very large strains. On the other hand, individual carbon nanotubes could exceed GFs >1000 at large strains, and >100 at low strains [1]. Besides lower power consumption, strain gauges based on individual-CNTs, having a larger GF at low strain levels, could be employed in applications where strains are not that large, e.g. on the thorax.

Description of the New Method

In this work we present a new respiration activity patch (RAP) concept based on individual-CNT strain gauges. The concept shown in Fig. 1 consists of a MEMS device with two movable sides connected by springs, and two CNT strain gauges. The MEMS device is adhered to a stretchable PDMS patch and connected electrically to two flat flexible cables (FFCs). Details on the fabrication process of the MEMS device and the CNT dry-transfer are given in [3].

The MEMS devices suffer distortions upon transfer onto the soft PDMS substrate. As exemplified

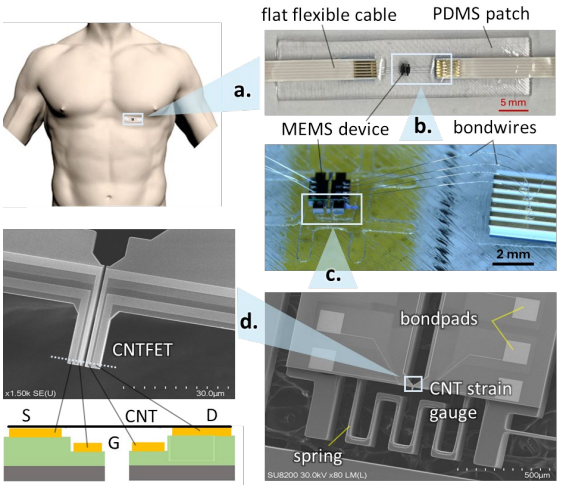

Fig. 1. Overview of the respiratory activity patch (RAP), from thorax placement (top-left) to schematic representation of the carbon nanotube (CNT) strain gauge (bottom-left). (a,b) Optical, (c,d) SEM images of the MEMS device and the CNT field effect transistor (CNTFET). (a-d) Images from different samples.

in Fig. 2 this leads to sloping and offsets between the two sides of the MEMS, which increases the CNT dry-transfer difficulty. However, white light interferometer (WLI) images are useful to select devices for further CNT transfer that show minimal deformations.

A key figure of the RAP mechanical behavior is the leverage factor η, defined as the ratio of the CNT elongation δl to the PDMS patch deformation ΔL (between FFCs). Its value was determined in two ways. First, η was extracted from Comsol Multiphysics simulations. This was necessary because the soft-hard PDMS-silicon interfaces result in non-trivial deformation fields, making an analytical derivation of η impossible.

Second, η was determined experimentally with a dedicated straining setup with piezoelectric actuation that fits under the WLI.

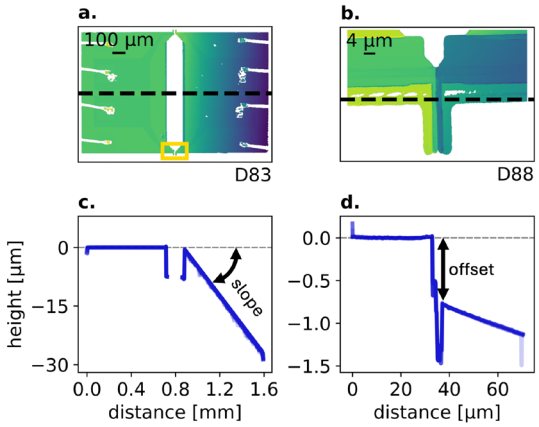

Fig. 2. WLI analysis of two different RAP devices. (a,c) Whole MEMS chip area and (b,d) close-up to the CNT electrode region. (a,b) Top-view WLI images and (c,d) slice plots at dashed lines in (a,b) respectively.

Results

In Fig. 3 a typical simulated mechanical deformation of a uniaxially strained RAP is shown for a MEMS device with a 3-fold spring design. The values of η extracted from simulation vary depending on the spring design (3 vs 5-fold), patch thickness (1.3 vs 2.2 mm) and PDMS E-modulus (1.5 vs 4.5 MPa), in the range 1.5-6.64 nm/µm. This range can be exploited in the future for customizing the sensitivity of the RAP to a specific use-case. Two measured devices are shown in Fig. 3.b. One of the two devices shows an η value of 1.25 nm/µm (3-fold spring) and the other

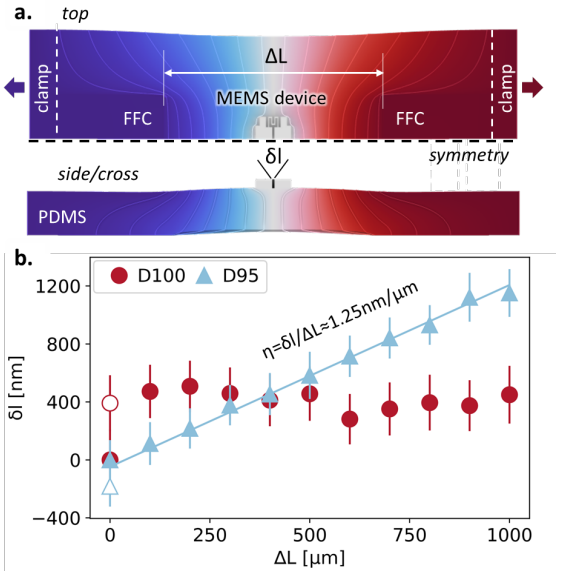

Fig. 3. Determination of the leverage factor η, via (a) Comsol mechanics simulations of the RAP deformation and (b) WLI imaging of two different RAPs characterized mechanically in a piezo-actuated setup.

(1-fold spring) shows no discernable response. Simulations and experiments agree about the order of magnitude of η. Future improvements in the placement precision of the MEMS devices onto the PDMS, and PDMS thickness control should improve the agreement. Fig. 4. shows additional analysis based on WLI of the evolution of the slope and the electrode vertical offset during straining. While large offsets could lead to CNT shorts to the gate electrode, the slope might influence strain levels and sensitivity. Besides revealing the complex mechanical interaction between the MEMS device and the PDMS support, these results suggest that pre-straining the patches can remove undesired initial slopes and offsets.

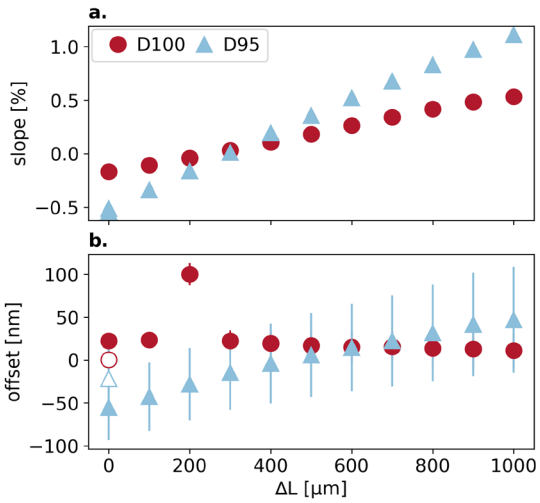

Fig. 4. Experimental determination from WLI images of the evolution of (a) slope and (b) offset mechanical distortions during uniaxial straining of the patch.

This work is a first demonstration of integrating a solid-state CNT strain gauge onto a soft, stretchable PDMS patch, and overcoming challenges stemming from hard-soft material interfaces.

References

[1] T. Helbling, C. Roman, L. Durrer, C. Stampfer, and C. Hierold, *IEEE TED* 58, 4053-4060 (2011); doi: 10.1109/TED.2011.2165544

[2] X. Wang, J .Li, H. Song, H. Huang, and J. Gou, *ACS Appl. Mats. & Interfaces* 10, 7371-7380 (2018); doi: 10.1021/acsami.7b17766

[3] M. Vollmann, C. Roman, M. Haluska, and C. Hierold, *IEEE MEMS Conference 2023*; doi: 10.1109/MEMS49605.2023.10052187

Acknowledgements

We thank the BRNC, CMi and First-CLA Cleanrooms, and in particular U. Drechsler, M. Haluska, H. ben Lakhdar, L. Maini for their help and support. This work has been supported by the European Union's Horizon 2020 research and innovation program under grant agreement no. 101017915 (DIGIPREDICT).